Q. J. R. Meteorol. Soc. (1996), **122**, pp. 1873–1890

A line-by-line investigation of solar radiative effects in vertically inhomogeneous low clouds

By V. RAMASWAMY* and J. LI
Princeton University, USA

(Received 21 September 1995; revised 1 April 1996)

SUMMARY

Using a detailed line-by-line, multiple-scattering solar radiative-transfer model, the influences due to cloud internal inhomogeneity in the vertical upon the solar radiative transfer are investigated. In particular, the consequences due to non-uniform vertical profiles of liquid water and droplet sizes within low clouds are explored in a systematic manner. The fine structure of the spectral overlap between the water droplet and water vapour optical properties, and its effects upon the radiation absorbed within the cloud layer and that reflected at the top of the cloud, are discussed. Without consideration of the in-cloud water vapour, a vertically inhomogeneous cloud with properties resembling those observed absorbs more solar radiation than an equivalent homogeneous cloud. However, consideration of the effects of the in-cloud vapour, while still leading to a slightly greater absorption for the inhomogeneous case, partly offsets the difference introduced by the vertical distribution of the drop microphysics. The vertical distribution of cloud heating rate is changed substantially because of the inhomogeneity in the microphysics, with the heating rate in the top region of the cloud nearly 50% more than that due to an equivalent vertically homogeneous cloud. Vertical inhomogeneity of cloud microphysics has little influence on the broadband solar albedo, but can cause significant decreases of the cloud reflectance at specific near-infrared wavelengths i.e. wavelengths greater than 1 μm, (equivalently, wave numbers less than 10 000 cm^{-1}).

KEYWORDS: Cloud optical properties Inhomogeneous cloud Radiative-transfer model Solar-radiation scattering

1. INTRODUCTION

Both climate and climate change are intimately related to the earth's solar-radiation budget, which in turn is strongly influenced by clouds. The solar radiative interactions depend to a considerable extent on the cloud geometric structure and cloud internal optical properties, both of which could give rise to significantly different effects than the assumption of plane-parallel, homogeneous clouds with infinite horizontal extent. In the last two decades, the effects of finite clouds on radiative transfer have been intensively studied through Monte Carlo simulations (McKee and Cox 1974; Davies 1978; Welch and Wielicki 1985; Barker and Davies 1992; and others). Li *et al.* (1994) considered a Monte Carlo model in which the effect of cloud microphysics with spatially varying single-scattering properties was employed. It is found that in cases when the cloud amount is large, inhomogeneous clouds lead to an increase in cloud solar absorption, which may be one factor to consider in the cloud absorption anomaly problem (Stephens and Tsay 1990).

An important factor in the solar radiative interactions with clouds is the presence of gaseous absorbers, notably water vapour above and inside the cloud. The studies of Davies *et al.* (1984) and Ramaswamy and Freidenreich (1992) emphasize that the spectral overlap between water vapour and droplets possesses a very fine structure and is of significant quantitative importance in determining the absorption in cloudy atmospheres.

As a step towards understanding the effects of inhomogeneity in clouds, we consider the problem of low clouds in which there is a vertical variation of the drop microphysics. The internal vertical distribution of the drop characteristics effectively yields a vertically inhomogeneous cloud. The principal objective here is to analyse systematically the influence due to the vertical inhomogeneity upon the spectrally dependent solar radiative transfer. The focus here differs somewhat from that in the study by Wiscombe *et al.* (1984)

* Corresponding author: NOAA Geophysical Fluid Dynamics Laboratory, Princeton University, PO Box 308, Princeton, NJ 08542, USA.

who examined the radiative roles of large cloud drops. For our purposes, we use the Geophysical Fluid Dynamics Laboratory (GFDL) line-by-line, multiple-scattering model (Ramaswamy and Freidenreich 1991) to perform the computations. The use of this model enables a high-resolution spectral investigation of the solar interactions with water vapour and droplets in inhomogeneous clouds, a feature that has been attempted only in a limited number of previous studies. The vertical variation of cloud microphysical properties is treated in a general manner guided by observational data on cloud microphysics, and the spectral analyses of cloud absorption and reflection at the top of the cloud are emphasized.

2. Model

(*a*) *Radiative transfer*

The GFDL solar line-by-line algorithm includes water vapour, carbon dioxide, and oxygen (Ramaswamy and Freidenreich 1991; Freidenreich and Ramaswamy 1993). The absorption spectra for these atmospheric gases are derived from the Air Force Geophysics Laboratory (AFGL) line parameter catalogue (Rothman *et al.* 1983). The average spectral resolution in the algorithm is about 3×10^{-3} cm^{-1}. Additional possible absorption due to water vapour continuum is not considered here. The absorption cross-sections of ozone follow the World Meteorological Organization (WMO) (1986). The solar spectrum considered in this study extends from 40 000 to 2500 cm^{-1} (or, equivalently, 0.25 to 4 μm), with approximately 3 million discrete frequency points.

In the atmosphere, multiple-scattering processes arise due to scattering by molecules (Rayleigh scattering) and cloud droplets. For a vertically inhomogeneous atmosphere, the precise method for dealing with the radiative transfer is the doubling and adding method (Hunt and Grant 1969; Coakley *et al.* 1983). The combination of the line-by-line and doubling-adding methods provides a highly accurate technique for evaluating the radiative fluxes and heating rates in a plane-parallel, absorbing–scattering atmosphere. However, this method is very time consuming, and can only be afforded in a few 'benchmark' calculations (Ramaswamy and Freidenreich 1991). Instead, as Ramaswamy and Freidenreich (1992) showed, the line-by-line algorithm can be combined with an approximate radiative-transfer method (e.g. δ-Eddington approximation) to ease the computational burden. Recently, a four-stream spherical harmonic expansion approximation method (four-stream SHEA, Li and Ramaswamy (1996)) has been formulated. In comparison with the δ-Eddington approximation, the four-stream SHEA yields much more accurate results for multiple scattering. For optical depths larger than one, the relative errors for reflection, transmission and absorption are, for the most part, less than 1%. Hence, for the calculations in this paper, the line-by-line technique for molecular absorption is combined with the four-stream SHEA for multiple scattering.

The column radiative-transfer model spans the pressure levels from the top of the atmosphere to the surface (1013 mb), and has 122 layers for distinguishing the inhomogeneous distribution of the atmospheric gases. Below the tropopause (100 mb), each layer is 20 mb thick (Ramaswamy and Freidenreich 1991). For the purposes of this study, if an inhomogeneous cloud exists in a 20 mb layer, that particular layer is divided into five sub-layers of equal pressure thickness, thereby resolving the cloud vertical structure in considerable detail. For all the computations in this paper, the cloud is placed between 800 and 900 mb. We consider the cloud to be embedded in a tropical atmospheric profile (McClatchey *et al.* 1972) for most of the calculations, and discuss briefly the differences when the cloud is placed in a mid-latitude summer atmosphere. Water vapour inside the cloud layers is assumed to be at saturation values corresponding to the local temperature,

while the vapour above the cloud in all the computations is accounted for according to the atmospheric profile assumed.

(*b*) *Cloud microphysical properties*

In contrast to the very fine spectral structure of water vapour, the radiative property of water droplets is uniform over relatively broad frequency intervals (Davies *et al.* 1984; Ramaswamy and Freidenreich 1992). One could, in principle, use Mie-scattering theory to determine the single-scattering properties of the water drops considered here. However, because of variations in cloud internal microphysics, the single-scattering calculations need to be performed not only for the different spectral frequencies but also for the varying droplet size distributions from cloud base to top. This would require too many Mie calculations, which is computationally burdensome. Instead, a more economical way is to relate the cloud optical properties to the cloud microphysical properties through a parametrization. We use here the Slingo (1989) 24-band parametrization for water clouds. This parametrization expresses the single-scattering properties as a function of cloud liquid-water content (LWC) and effective radius, r_e. For the 4-stream multiple-scattering calculations, the two higher moments in phase function are obtained by Mie solutions using a modified gamma size distribution. The single-scattering properties are assumed to be constant within each band. Thus, each discrete frequency point within a specific band is assigned the same value of the single-scattering property.

There are a number of observations illustrating the vertical distribution of cloud LWC for water clouds (Paltridge 1974; Platt 1976; Slingo *et al.* 1982a, b; Noonkester 1984; Stephens and Platt 1987; and the early measurements summarized by Mason (1971)). All these observations show that, inside stratus and stratocumulus clouds, the cloud LWC increases nearly linearly with height from cloud base. Most of these observations are restricted to LWC only. However, the spatial variation of r_e has been reported by Noonkester (1984) and Stephens and Platt (1987).

LWC and r_e are not independent of each other, and the relation between them can be derived in a general manner. We assume that the cloud droplet size distribution conforms to a modified gamma distribution

$$n(r) = Ar^{\alpha}e^{-\beta r}, \tag{1}$$

where r is the radius of the droplet; A, α and β are positive constants.

The total number concentration of the droplets is given by

$$N = \int n(r)\ \mathrm{d}r = \frac{A\Gamma(\alpha+1)}{\beta^{\alpha+1}}, \tag{2}$$

where Γ is the gamma function. LWC and r_e are determined by

$$r_e = \frac{\int r^3 n(r)\ \mathrm{d}r}{\int r^2 n(r)\ \mathrm{d}r} = \frac{\alpha+3}{\beta} \tag{3}$$

and

$$w = \frac{4\pi}{3}\rho \int r^3 n(r)\ \mathrm{d}r = \frac{4\pi}{3}\rho N r_e^3 \frac{(\alpha+1)(\alpha+2)}{(\alpha+3)^2}, \tag{4}$$

where ρ is the density of liquid water. From Eq. (4), the relation between r_e and LWC is given by

$$r_e = f(\alpha)\left(\frac{3}{4\pi}\frac{w}{\rho N}\right)^{\frac{1}{3}}, \tag{5}$$

where the factor $f(\alpha) = \{(\alpha+3)^2/(\alpha+1)(\alpha+2)\}^{\frac{1}{3}}$. $f(\alpha)$ approaches unity for large values of α, and is constrained to be less than 1.65 ($f(0) = 1.65$). Considering the cloud types Sc1 and Sc2 (Stephens 1978), though these cloud size distributions are quite different, the values of $f(\alpha)$ are confined to between 1.09 and 1.11. This indicates that $f(\alpha)$ is approximately a constant for the various size distributions. We therefore simply take $f(\alpha) = 1.1$ in the following calculations. From Eq. (5), the spatial variation of r_e can be determined through the spatial variations of w and N. Earlier, Twomey has also found that r_e is proportional to $(w/N)^{\frac{1}{3}}$ (Coakley *et al.* 1988).

The values of LWC at the base of the clouds are usually quite small. In the following, therefore, we take the value of LWC at the base of a cloud to be 0.01 g m^{-3}, and assume the LWC to increase linearly inside the cloud. Then, the slope, or the rate of increase of LWC with height, is determined by the vertically averaged value of LWC assumed.

Though both the LWC and r_e increase with height inside the boundary-layer clouds, the number concentration of the cloud droplets does not show such a tendency, according to the observations of Stephens and Platt (1987). For a boundary-layer cloud, if there is a reasonable degree of convective mixing, the cloud droplet concentration can be expected to be uniform throughout the cloud, since probably all the cloud concentration nuclei (CCN) that can be activated do so at cloud base, and there are not many new CCN because entrainment from cloud top is usually weak in boundary-layer clouds. Therefore N can be assumed to be nearly constant with height. This can be verified by two of the three results in Stephens and Platt (1987). Therefore, in the following, we adopt, for the most part, a vertically uniform value for the number concentration. We will, however, consider the vertical variation of concentration with height (i.e. different slopes) in order to illustrate its influence on the radiative transfer. The slope of the vertical variation of volume concentration is defined as

$$\eta = \frac{N_t - N_b}{N_t + N_b} \tag{6}$$

where N_t and N_b are the values of the volume concentration of the droplets at the cloud top and the cloud base, respectively. $\eta = 0$ corresponds to the case of a constant value of the volume concentration with height, while a large positive value corresponds to a relatively greater concentration at the cloud top than at cloud base. The vertically averaged value of the number concentration is $\langle N \rangle = (N_t + N_b)/2$.

In Fig. 1, the vertical profiles of r_e are shown for different vertical variations of droplet distribution. It is to be noted that the prescription of cloud drop microphysics here differs considerably from earlier studies (e.g. Wiscombe *et al.* 1984). In Fig. 1(a), the LWC increases linearly with height with a vertically averaged value $\langle w \rangle = 0.2$ g m^{-3}, while N is assumed to be uniform throughout the cloud. It is seen that r_e increases with height more rapidly for a smaller value of N (see Eq. (5)). In Fig. 1(b), the vertical profile of the LWC is the same as in Fig. 1(a) while $\langle N \rangle = 100$ cm^{-3}. From Fig. 1(b), r_e is seen to be smaller in the upper region of the cloud for an increasing positive value of η. In Fig. 1(c), the vertical variations of r_e due to different values of $\langle w \rangle$ are illustrated, with the droplet concentration held constant at 50 cm^{-3}. It is apparent that r_e increases with height in a very significant manner for a larger value of the vertically averaged LWC.

3. Numerical results and discussions

(a) *Cloud absorption*

We consider first the spectral distribution of absorption in a cloud layer without water vapour (and other atmospheric gases) inside it. The plane-parallel cloud considered (800

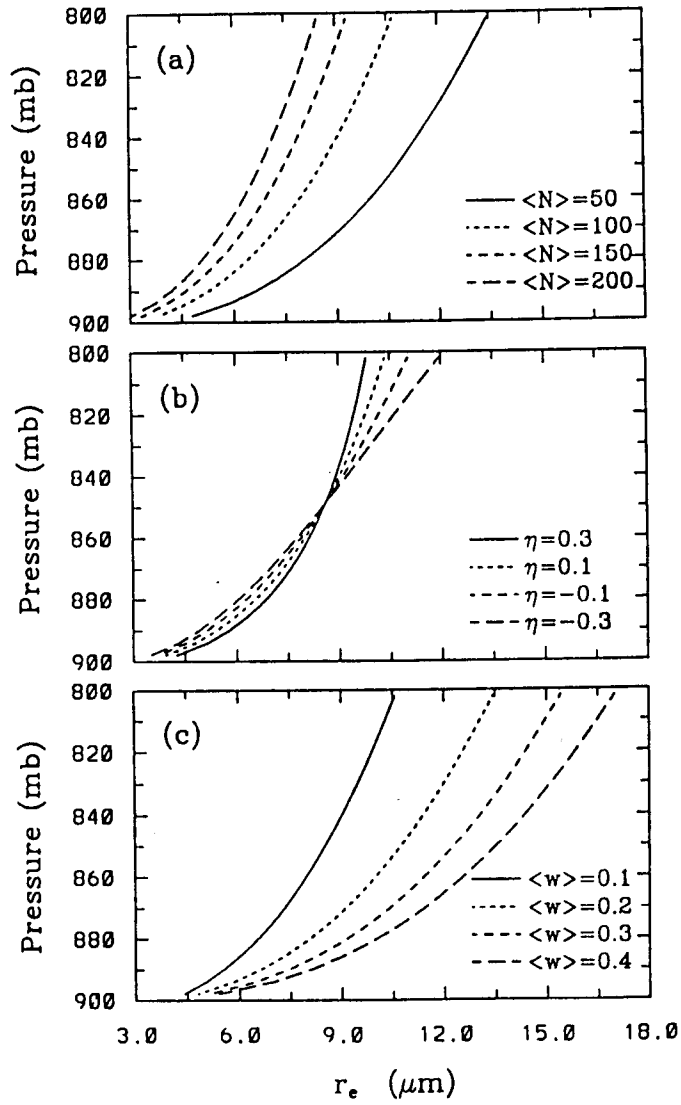

Figure 1. Vertical variation of the effective radius, r_e. (a) Profiles of r_e for different values of volume concentration, $\langle N \rangle$; number concentration is uniform throughout the cloud. Liquid-water content (LWC) increases linearly in altitude, with a vertically averaged value $\langle w \rangle = 0.2$ (g m^{-3}). (b) Profiles of r_e with different values of the vertical slope of the number concentration, η; the vertically averaged number concentration $\langle N \rangle = 100$ (cm^{-3}); LWC is the same as that in (a). (c) Profiles of r_e for different values of $\langle w \rangle$; LWC increases linearly with altitude, and number concentration is constant with $\langle N \rangle = 50$ (cm^{-3}).

to 900 mb) has LWC equal to 0.2 g m^{-3}, a typical value for stratus and stratocumulus clouds (McKee and Cox 1974). For a vertically inhomogeneous cloud, the LWC increases linearly in altitude, with the cloud base value (w_b) being 0.01 g m^{-3}. The value of $\langle w \rangle$ in the inhomogeneous cloud is the same as that for its homogeneous counterpart. Note that the equivalence of LWC between the homogeneous and the inhomogeneous clouds is different from assuming an equivalence of the extinction optical depth (the difference is usually small).

In Stephens (1978), the cloud volume concentrations were 350 cm^{-3} and 150 cm^{-3} for the Sc1 and Sc2 cloud models, respectively. However, later observations show a lesser value for the droplet concentration (Stephens and Platt 1987), with stratocumulus clouds having, on average, a volume concentration of about 50 cm^{-3}. Here, we take N to be constant at 50 cm^{-3} for both the homogeneous and inhomogeneous cases. The sensitivity to the value assumed for the volume concentration will be discussed subsequently. The

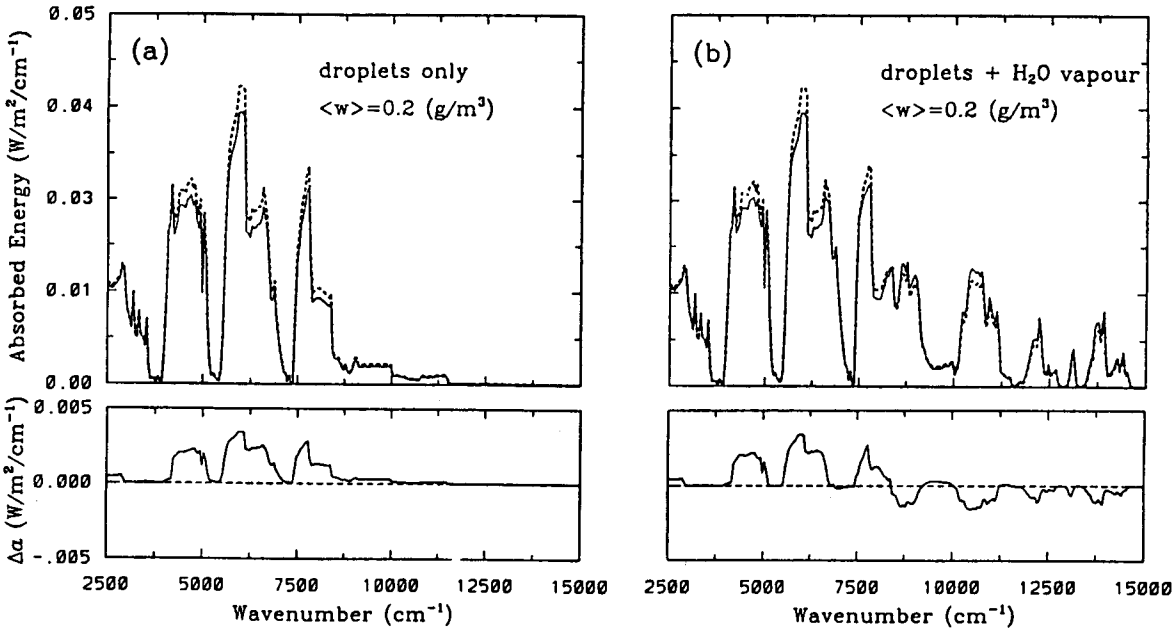

Figure 2. (a) Spectral absorption by the vertically inhomogeneous cloud (dotted line) and its homogeneous counterpart (solid line). Only droplets inside the cloud are considered and in-cloud water vapour is ignored. $\langle w \rangle = 0.2$ (g m^{-3}), $\langle N \rangle = 50$ (cm^{-3}) and $\theta_0 = 0°$ (see text for explanation of symbols). The upper panel illustrates the spectral absorption while the lower panel is the difference ($\Delta\alpha$) in spectral absorption between the inhomogeneous cloud and its homogeneous counterpart. (b) Same as (a), with water vapour (and other atmospheric gases) included in the cloud layer.

corresponding vertical variation of r_e can be found from Eq. (5) and is shown in Fig. 1(a). The vertically averaged value of r_e is 10.8 μm. The cloud is placed in a standard tropical atmosphere with a surface albedo of 0.1, while the solar zenith angle $\theta_0 = 0°$.

The spectral distribution of absorption by the cloud layer is shown in Fig. 2(a). We plot only the spectral range from 2500 cm^{-1} to 15 000 cm^{-1} (in wavelength space, this corresponds to the range from 4 to 0.67 μm). Beyond 15 000 cm^{-1} the cloud droplet absorption becomes very weak. Though the results are obtained for each discrete frequency, the curves in Fig. 2(a) are plotted as averages over every 50 cm^{-1}. The corresponding lower panels illustrate the differences in the spectral absorption ($\Delta\alpha$) between the inhomogeneous and homogeneous cases. As expected, a strong absorption occurs for wave numbers less than 10 000 cm^{-1}. Also, over most of the spectral region, the cloud vertical inhomogeneity enhances the cloud absorption.

In order to explain the physics of the enhancement of cloud absorption for the inhomogeneous cloud, we plot in Fig. 3 the vertical variation of cloud optical properties corresponding to the vertically inhomogeneous cloud in Fig. 2(a). The cloud optical properties (i.e. extinction coefficient, single-scattering albedo and asymmetry factor) are dependent on wavelength. Only two groups of values for bands 0.52–0.57 μm and 1.64–2.13 μm (cf. Slingo 1989) are plotted in Fig. 3; these bands are located in the visible and near-infrared regions, respectively. (In wave-number space, these spectral regions correspond to 19 231–17 544 and 6098–4695 cm^{-1}, respectively). It is shown in Fig. 3 that, for a vertically inhomogeneous cloud, the upper part of the cloud corresponds to a larger extinction coefficient and a smaller single-scattering albedo. This is because of a relatively larger LWC and r_e there (see Fig. 1). Therefore, near cloud top, more scattering events occur, accompanied by a higher absorption in the near-infrared, which causes an increase in cloud absorption in the inhomogeneous case compared with the homogeneous one. For either case, most of the absorption takes place within the top half of the cloud.

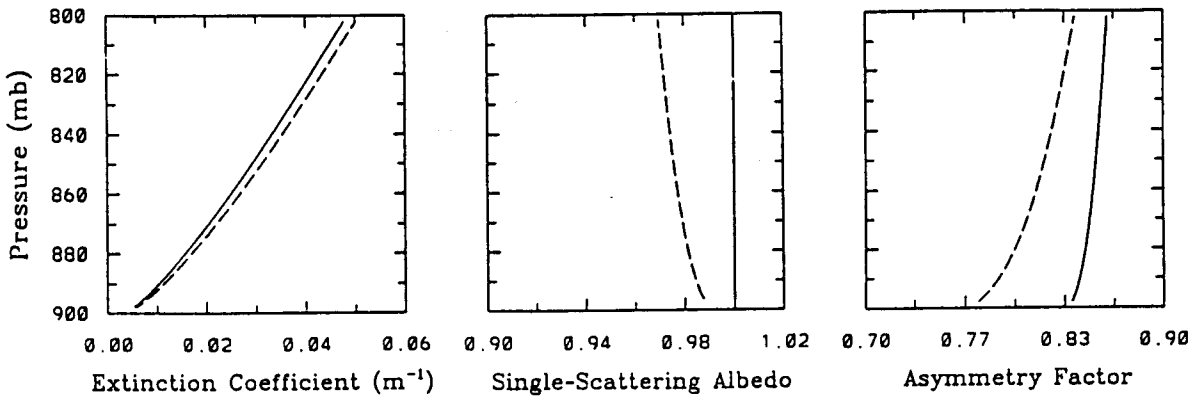

Figure 3. Vertical profiles of the drop single-scattering properties within the inhomogeneous cloud employed in Fig. 2(a). Two bands, viz. 0.52–0.57 μm (solid line) and 1.64–2.13 μm (dashed line), are considered.

In Fig. 2(b) the cloud case is the same as that in Fig. 2(a) except that water vapour (at saturation value), along with other atmospheric gases, is included inside the cloud layer. The other gases, viz. carbon dioxide, oxygen and ozone, play a negligible role compared with water vapour. Beyond 15 000 cm^{-1}, both water droplet and water vapour have very small absorption. In comparison with Fig. 2(a) and consistent with Davies *et al.* (1984), we find the water vapour inside the cloud to have a significant absorption in the region between 8000 cm^{-1} (1.25 μm) and 15 000 cm^{-1} (0.67 μm). This is in contrast to the situation for the water droplet absorption, which occurs at smaller wave numbers (less than 8000 cm^{-1}). The overlap of absorption between water droplet and water vapour is strong only in a narrow region near 8000–10 000 cm^{-1}.

It is also interesting to find in Fig. 2(b) that, beyond 8000 cm^{-1} (i.e. in the water vapour absorption-dominated region), the situation is opposite to that of the water droplet absorption-dominated region (wave number less than 8000 cm^{-1}), in that the vertically inhomogeneous cloud absorbs less solar radiative energy in comparison with its homogeneous counterpart. This feature due to water vapour largely offsets the effect of enhancement in the cloud absorption caused by the vertical inhomogeneous distribution of cloud droplets, shown in Fig. 2(a). In Fig. 4, the frequency-accumulated cloud absorption over the solar spectrum is shown for both cloud droplet only and cloud droplet-plus-vapour cases. In the case of cloud droplet only, the accumulated absorption assumes a nearly constant value for wave numbers larger than 8000 cm^{-1}, since the absorption by droplet becomes very weak over this spectral region. We find that the vertical inhomogeneity, by itself, can cause about a 10% increase in cloud spectrally integrated absorption. With the inclusion of water vapour, the difference in the accumulated absorption between the inhomogeneous cloud and its homogeneous counterpart becomes less than the corresponding result for the droplet-only cloud, which clearly demonstrates the offsetting effect brought about by water vapour towards the total cloud absorption. For the solar spectrum as a whole, the inhomogeneous case absorption is seen to exceed that of its homogeneous counterpart.

In the water vapour absorption-dominated region (wave numbers greater than 8000 cm^{-1}), the cloud water-droplet absorption is very weak (Fig. 2(a)). Therefore, any enhancement of absorption due to inhomogeneity in the single-scattering albedo is necessarily small in this spectral region. On the other hand, for a vertically inhomogeneous cloud, the relatively larger asymmetry factor in the upper part of the cloud (Fig. 3) results in the scattered photons having a greater tendency to go downward. On average, thus, the path length for a photon in the upper part of the inhomogeneous cloud is reduced in comparison with the homogeneous case. Since the water vapour absorption is proportional

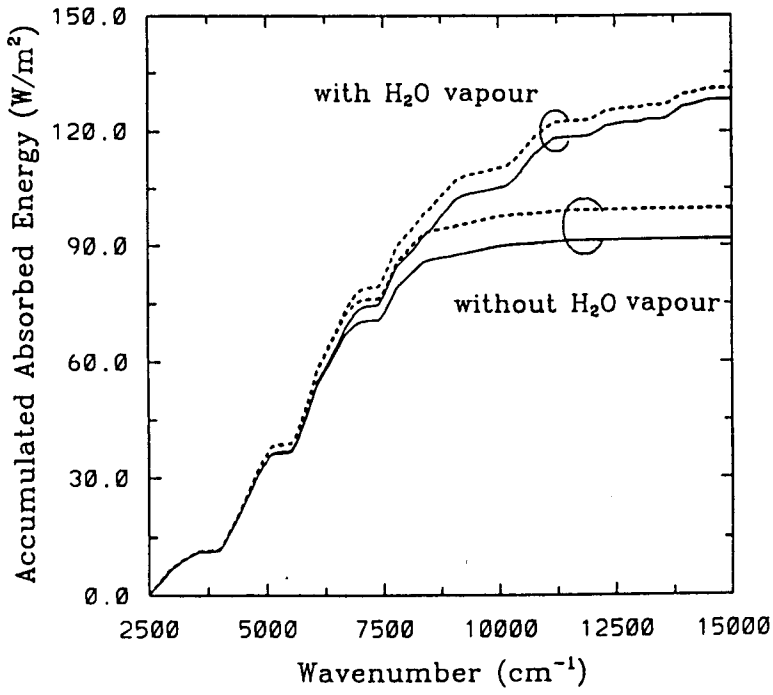

Figure 4. Frequency-dependent cumulative cloud absorption corresponding to the cloud case in Fig. 2(a) (droplet only) and that corresponding to the cloud case in Fig. 2(b) (droplet plus water vapour and other atmospheric gases inside cloud). Both vertically homogeneous (solid lines) and inhomogeneous (dashed lines) clouds are considered.

to the path length of the photons, there is a decrease in the water vapour absorption in the inhomogeneous case relative to the homogeneous one. In the lower part of the cloud, the inhomogeneous cloud has a smaller asymmetry factor in comparison with the homogeneous case, and the scattered photons are oriented more isotropically. However, this part of the cloud also has a smaller extinction coefficient; hence, the number of scattering events is small and the path length of the photon does not increase. Taking into account the entire cloud, the vertical inhomogeneity can be expected to lead to a shorter photon path length on average, and consequently the role of water vapour absorption in the entire cloud layer is less compared with the homogeneous case.

The results in Figs. 2(a) and (b) emphasize the importance of the radiative interactions with both water droplet and water vapour. One implication from the present results is that, for several of the earlier finite cloud studies, where water vapour effects (in and above cloud) were generally not considered in detail, the discussions may not be complete and there could be shortcomings in the quantitative estimates.

The vertically integrated absorptance by the cloud layer for different θ_0 is shown in Fig. 5. Both the in-cloud water vapour inclusion and exclusion cases are considered. For all zenith angles, the difference in absorption between the vertically inhomogeneous cloud and its homogeneous counterpart is much reduced when in-cloud water vapour is accounted for. Figure 5 shows that the difference introduced by the cloud internal vertical inhomogeneity is relatively insensitive to θ_0.

Figure 6 shows the influences of altitudinal variations in cloud microphysical properties (as illustrated in Fig. 1) upon the spectrally integrated cloud absorptance, with the water vapour absorption included. Figure 6(a) corresponds to the configurations shown in Fig. 1(a) and considers different number concentrations of cloud droplets. For the same value of LWC, an increase in cloud number concentration will decrease the cloud absorption. This is because the increase in N leads to a reduction in droplet r_e and, therefore, the

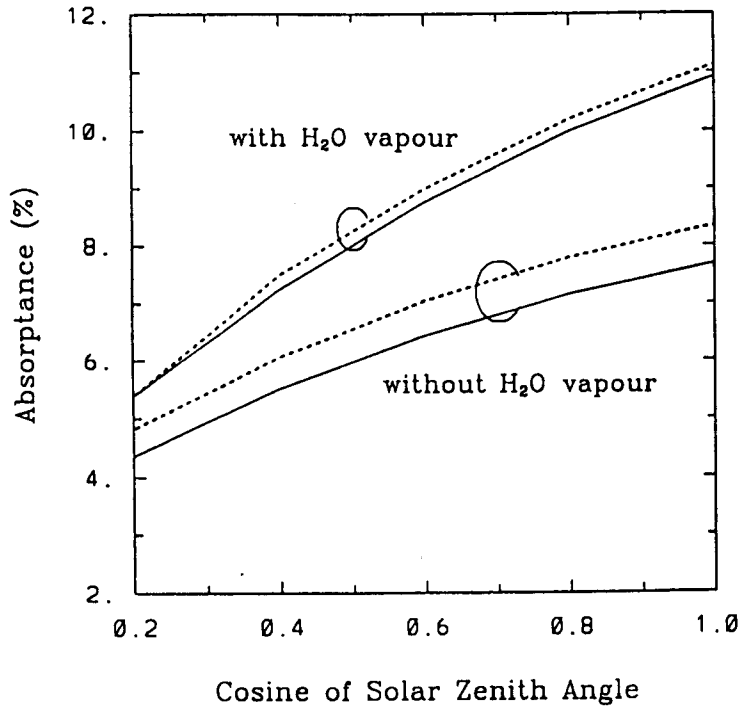

Figure 5. Spectrally integrated (0.25–4 μm) cloud absorption for different solar zenith angles, corresponding to the cloud cases in Fig. 2. Both vertically homogeneous (solid lines) and inhomogeneous (dashed lines) clouds are considered.

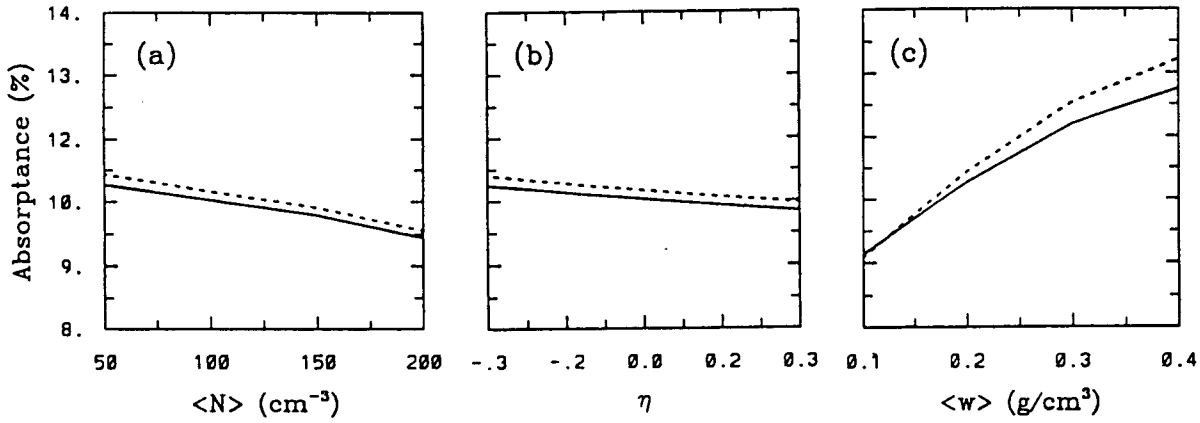

Figure 6. Spectrally integrated (0.25–4 μm) cloud absorption for the cloud cases shown in Figs. 1(a), 1(b) and 1(c), respectively. Both vertically homogeneous (solid lines) and inhomogeneous (dashed lines) clouds are considered.

single-scattering albedo increases. In Fig. 6(a) the inhomogeneous cloud always absorbs more radiative energy in comparison with its homogeneous counterpart; this is mostly due to the relatively larger r_e in the upper part, as discussed previously.

Figure 6(b) corresponds to the configurations shown in Fig. 1(b) and considers the vertical variation in the number concentration. The vertically averaged number concentration is kept the same. The spectrally integrated absorption by the cloud decreases with increase in the value of the slope, η. The larger the value of the slope, the more the droplet numbers in the upper part of the cloud. Therefore, r_e decreases and the single-scattering albedo increases in this region. The cloud absorption largely depends on the upper region

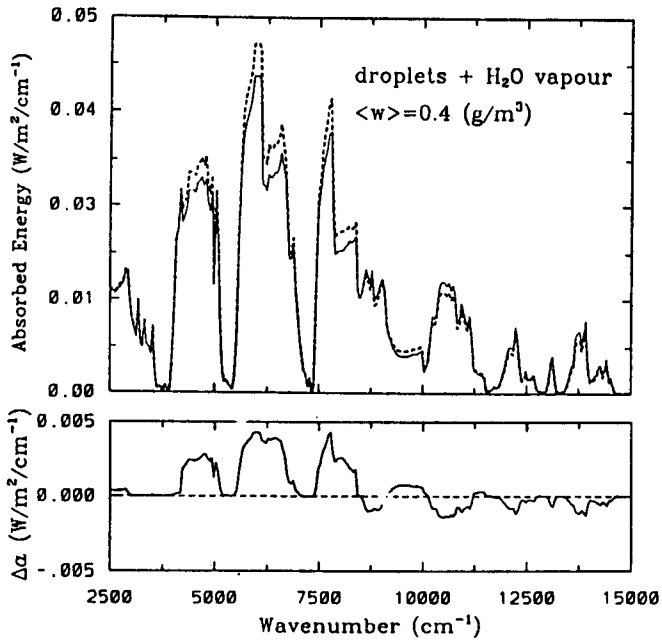

Figure 7. Spectral absorption by the vertically inhomogeneous cloud (dotted line) and its homogeneous counterpart (solid line), with water vapour included in the cloud layers. $\langle w \rangle = 0.4$ (g m^{-3}), $\langle N \rangle = 50$ (cm^{-3}) and $\theta_0 = 0°$ (see text for explanation of symbols). The upper panel illustrates the spectral absorption and the lower panel the difference ($\Delta\alpha$) in the spectral absorption between the inhomogeneous cloud and its homogeneous counterpart.

of the cloud, since most of solar energy is absorbed near the top (this is elaborated upon later in the text).

Finally we discuss Fig. 6(c) which corresponds to the cloud cases shown in Fig. 1(c). With an increase in $\langle w \rangle$, the cloud absorption increases. Also, the difference between the inhomogeneous cloud and its plane-parallel counterpart increases, which is unlike the behaviour seen in Figs. 6(a) and (b). In Fig. 6(c), when $\langle w \rangle$ is 0.1 g m^{-3}, there is no difference between the inhomogeneous cloud and its homogeneous counterpart. This shows that the enhanced absorption due to the vertically inhomogeneous distribution of the droplets is totally compensated by the offsetting effect of water vapour mentioned above. However, for a relatively large value of $\langle w \rangle$, the slope of w becomes greater, and, from Fig. 1(c), the difference in the vertical profile of r_e between the inhomogeneous cloud and its homogeneous counterpart becomes larger. Therefore, the enhancement in absorption due to the inhomogeneous distribution of droplets becomes greater, and this cannot be totally offset by the consideration of in-cloud water vapour. To verify this point, a spectral absorption plot, shown in Fig. 7 for $\langle w \rangle$ equal to 0.4 g m^{-3}, with the other cloud microphysical properties being the same as those for Fig. 2(b). We find that the difference between the inhomogeneous cloud and its homogeneous counterpart is enhanced in the droplet-dominated region (wave numbers less than 8000 cm^{-1}), relative to the result for the smaller $\langle w \rangle$ case shown in Fig. 2(b). However, the situation in the spectral region dominated by water vapour remains similar to that in Fig. 2(b), consistent with the physical effects outlined earlier.

From Fig. 6 it is concluded that the variations in the number concentration and its vertical slope have negligible influence on the difference in the spectrally integrated absorption between the inhomogeneous cloud and its homogeneous counterpart. For the wide variety of conditions examined, the absorption by the vertically inhomogeneous cloud exceeds that by the equivalent homogeneous one.

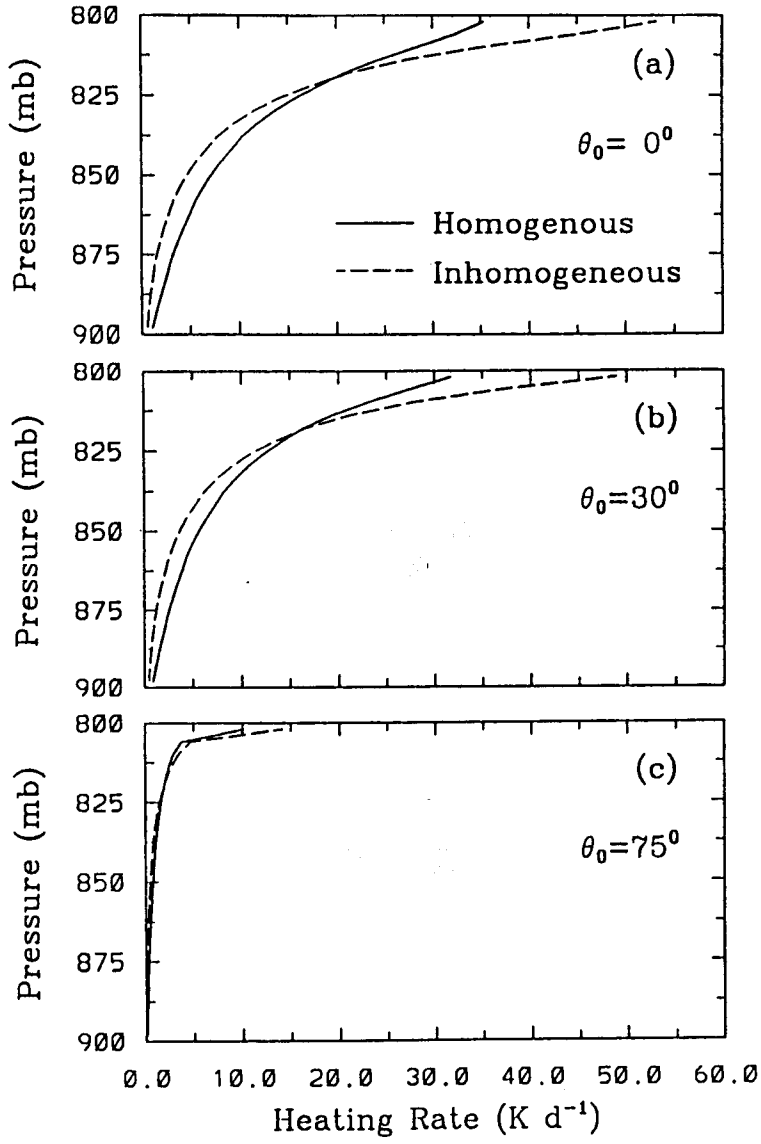

Figure 8. Vertical distributions of the heating rates inside the cloud layer for solar zenith angles of (a) 0°, (b) 30° and (c) 75°. The cloud case is the same as that in Fig. 2(b). Both vertically homogeneous and inhomogeneous clouds are considered.

The vertical distribution of the spectrally integrated absorption inside the cloud is shown in Fig. 8. The cloud case is the same as that in Fig. 2(b). Three different solar zenith angles are considered. Though the vertically integrated value of absorption is very similar for the two cloud cases, because of the offsetting effect of water vapour stated earlier (see Fig. 4) Fig. 8 illustrates that the vertical distribution of the heating rate inside the cloud is significantly different between the inhomogeneous and homogeneous clouds. In particular, the heating rate in the inhomogeneous case is concentrated more in the top region of the cloud. When θ_0 is small, the heating rate near the cloud top for an inhomogeneous cloud can exceed that for the homogeneous cloud by nearly 50%. The enhancement for vertically inhomogeneous clouds could affect estimates of the relative roles of the solar and long-wave radiative energy disposition inside the clouds (Stephens 1978).

The distribution of solar heating rate is an important factor in cloud formation and maintenance. The solar heating rate in the upper part of a cloud would tend to suppress the convection process and stabilize the cloud layer. The finding of the relatively large

TABLE 1. WIDE-BAND ABSORPTION (W M^{-2}) BY VERTICALLY INHOMOGENEOUS CLOUD $\alpha(ih)$ AND ITS HOMOGENEOUS COUNTERPART $\alpha(h)$ IN TROPICAL AND MID-LATITUDE SUMMER ATMOSPHERES

	Tropics		Mid-latitude summer	
Band (cm^{-1})	2500–8000	8000–15 000	2500–8000	8000–15 000
Band (μm)	1.250–4.000	0.667–1.250	1.250–4.000	0.667–1.250
$\alpha(h)$	85.82	41.28	90.00	40.03
$\alpha(ih)$	91.32	38.60	95.67	37.56
$\Delta\alpha$	5.50	−2.68	5.67	−2.47

$\Delta\alpha = \alpha(ih) - \alpha(h)$. Cloud with $\langle w \rangle = 0.2$ (g m^{-3}), $\langle N \rangle = 50$ (cm^{-3}); $\theta_0 = 0°$ (see text for explanation of symbols).

distribution of heating rate near the top of a cloud with vertical inhomogeneity in the microphysics could be expected to affect the cloud evolution process, and is thus an important element to be taken into consideration in cloud modelling studies.

We have also performed computations for the same cloud cases using the mid-latitude summer profile (McClatchey *et al.* 1972), and with appropriate saturation values of water vapour within the cloud. It is found that the spectral absorption features are nearly similar to those for the tropical case above. Since the differences in the spectral results between the two atmospheric profiles turn out to be small, we compare the wide-band absorption features for the two profiles (Table 1). The offsetting effect of water vapour discussed earlier holds true for the mid-latitude summer case as well. Despite the differences in the moisture profile for the two standard atmospheres, the difference in absorption between the homogeneous and inhomogeneous cases is approximately similar for both atmospheres. Note, however, that, as is to be expected, the absorption by either the inhomogeneous or the homogeneous cloud differs between the tropical and mid-latitude summer conditions. While the calculations here are not exhaustive, they do suggest that the difference between the inhomogeneous and the equivalent homogeneous cloud absorption is not significantly influenced by the atmospheric profile assumed.

(*b*) *Decrease in the near-infrared albedo*

In the following, we investigate the spectral distribution of the cloud albedo in the vertically inhomogeneous cloud compared with its homogeneous counterpart. The motivation arises from Stephens and Tsay (1990), who point out that departures from theoretical estimates of the near-infrared cloud albedo, as inferred from observations (Hignett 1987), may be indicative of a cloud absorption anomaly.

Figure 9(a) shows the spectral distribution of cloud reflectance (spectral albedo) for the case corresponding to Fig. 2(b). We remind the reader that both the inhomogeneous and homogeneous calculations include considerations of the above-cloud water vapour absorption. The cloud reflectance is plotted as a function of wavelength (in microns) in order to refer to the results of Stephens and Tsay (1990). The solar spectral region considered extends from 0.25 to 4 μm (40 000–2500 cm^{-1}). In the visible region, as expected, there is nearly no difference between the reflectance of the inhomogeneous cloud and its homogeneous counterpart. However, in the near-infrared region, at wavelengths greater than 1 μm, the albedo of the vertically inhomogeneous cloud is significantly less in some spectral regions than estimated for the homogeneous case.

In order to understand physically why the difference in albedo occurs only in the near-infrared region, consider Fig. 3. There, it is shown that the asymmetry factor and single-scattering albedo for droplets are less sensitive to r_e in the visible region than in the

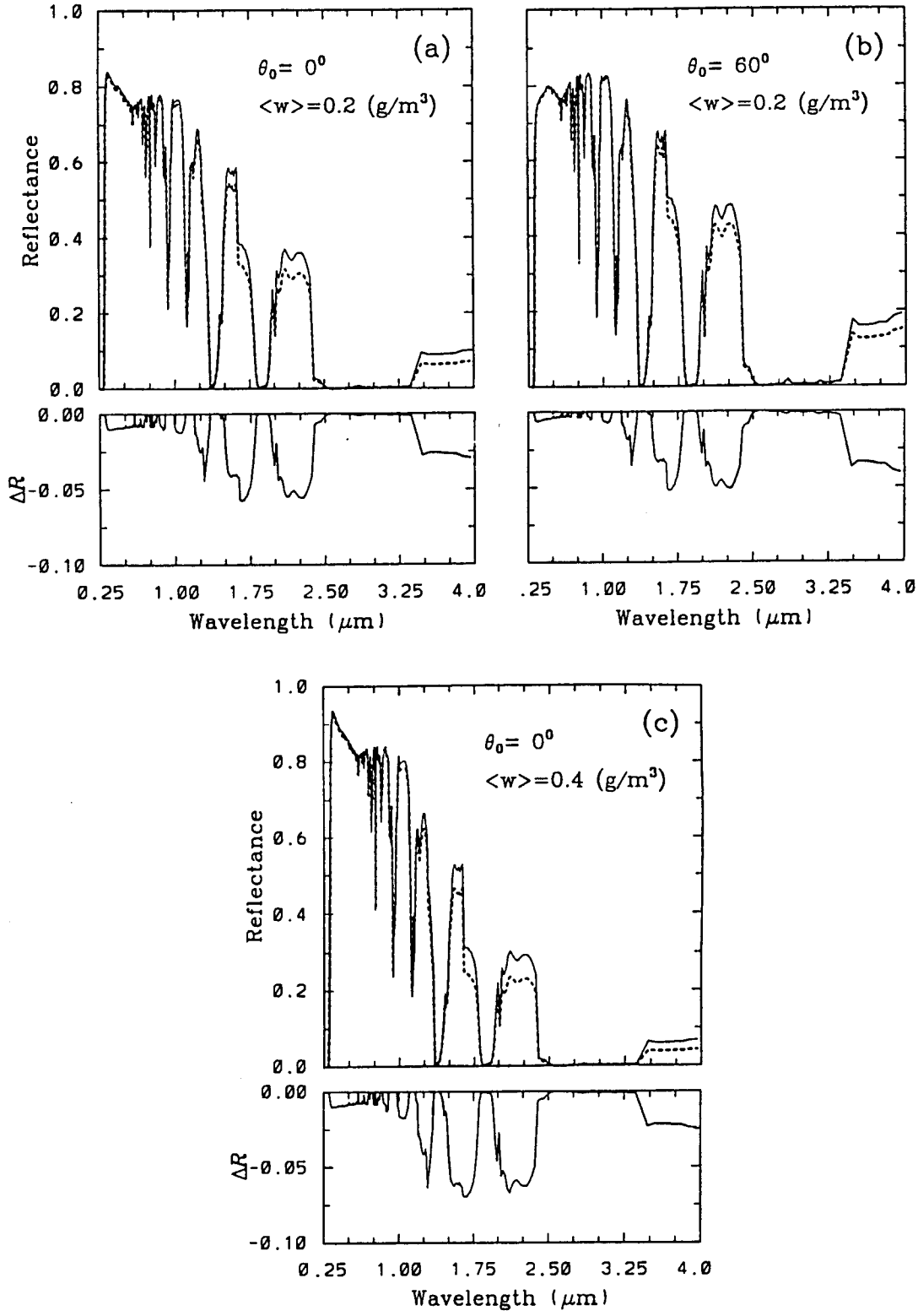

Figure 9. (a) Spectral albedo for an inhomogeneous cloud (dotted line) and its homogeneous counterpart (solid line), with water vapour included in the cloud layers. $\langle w \rangle = 0.2$ (g m^{-3}), $\langle N \rangle = 50$ (cm^{-3}) and $\theta_0 = 0°$ (see text for explanation of symbols). The upper panel illustrates the spectral reflectance and the lower panel the difference (ΔR) in the spectral reflectance between the inhomogeneous cloud and its homogeneous counterpart. (b) Same as (a), but with $\theta_0 = 60°$. (c) Same as (a), but with $\langle w \rangle = 0.4$ (g m^{-3}).

near-infrared region. If there are no variations in asymmetry factor and single-scattering albedo, the vertical variation of extinction coefficient alone would not lead to any difference in the radiative-transfer process when compared with the corresponding vertically averaged case (see Li *et al.* 1994). The presence of water vapour inside cloud would have no influence on the droplet asymmetry factor, but would influence the absorption coefficient and, hence, the layer single-scattering albedo (= 1 − absorption coefficient/extinction coefficient). However, the water vapour absorption in the visible region is very weak. Therefore, the vertical variations of asymmetry factor and single-scattering albedo within the cloud layer are small in the visible region in comparison with that in the near-infrared region, regardless of the presence of water vapour. Thus, the vertical inhomogeneity in cloud microphysics does not cause any apparent difference in the visible spectral reflectance.

In the near-infrared region, the upper part of the inhomogeneous cloud corresponds to a larger extinction coefficient, a smaller single-scattering albedo (Fig. 3), and a larger asymmetry factor in comparison with its homogeneous counterpart. Then, photons would have a greater probability of being absorbed (as manifest in the results shown in Fig. 2(b) and the discussions in the earlier section), while the non-absorbed photons would have a greater tendency to travel downward. In the lower part, for the inhomogeneous cloud, the asymmetry factor is smaller, but the smaller extinction coefficient in this region makes the number of scattering events relatively less. The non-absorbed photons would, on average, have an overall tendency to keep going in their downward direction. Therefore, the overall reflection by the cloud layer decreases. Although, in Fig. 3, only two bands of the cloud optical properties are shown, the physical situation in the other bands is similar, with a smaller vertical variation of the asymmetry factor in the visible regions and a larger vertical variation of the asymmetry factor in the near-infrared regions (see the value of the factor f_i in Table 1 of Slingo (1989)).

In Fig. 9(a), the decrease in near-infrared albedo for the vertically inhomogeneous cloud in the 0.75–1.25 μm (13 333–8000 cm^{-1}) spectral region is small. This may be attributed to the offsetting effect of water vapour in this spectral region (discussed in the previous section) and the relatively smaller vertical variation in the asymmetry factor (compared with that in the region of 1.25–4 μm (8000–2500 cm^{-1}); Slingo 1989).

The effect of a lesser infrared albedo for the inhomogeneous cloud relative to the homogeneous one is a result that holds regardless of θ_0. In Fig. 9(b), the cloud case is the same as that in Fig. 9(a), but the effect is shown for $\theta_0 = 60°$. Again, the difference in reflectance between the vertically inhomogeneous cloud and its homogeneous counterpart occurs mainly in the near-infrared region.

Figure 9(c) displays the spectral cloud reflectance for a cloud with a larger $\langle w \rangle$(= 0.4 g m^{-3}). Overhead sun condition is assumed in order to contrast the results with Fig. 9(a). Unlike the situation for absorption (Figs. 6 and 7), the larger value of $\langle w \rangle$ does not substantially enhance the albedo difference between the inhomogeneous cloud and its homogeneous counterpart in the near-infrared region.

In Fig. 9, the albedo differences between the vertically inhomogeneous clouds and their homogeneous counterpart occur mostly in the spectral region with wavelengths greater than 1 μm (wave numbers less than 10 000 cm^{-1}). Note that the solar irradiance decreases rapidly with increasing wavelength (or decreasing wave number) in this portion of the spectrum. Thus, if the near-infrared region is defined as extending from 0.75 μm to 4 μm (i.e. 13 333–2500 cm^{-1}), the difference in near-infrared albedo between the vertically inhomogeneous cloud and its homogeneous counterpart can be expected to be small. In Table 2 the albedos for visible (0.25–0.75 μm i.e. 40 000–13 333 cm^{-1}) and near-infrared (0.75–4 μm i.e. 13 333–2500 cm^{-1}) spectra are listed. Also listed are the ratios of the near-infrared to visible albedo for the vertically inhomogeneous and homogeneous cloud

TABLE 2. VISIBLE (0.25–0.75 μM) AND NEAR INFRARED (0.75–4 μM) ALBEDOS, AND THE RATIO OF NEAR-INFRARED TO VISIBLE ALBEDO FOR THE VERTICALLY INHOMOGENEOUS CLOUD AND ITS HOMOGENEOUS COUNTERPART (IN PARENTHESES)

Vertically averaged liquid-water content ($g\ m^{-3}$)	Visible	Near infrared	Ratio
0.1	0.675 (0.680)	0.576 (0.584)	0.853 (0.859)
0.2	0.758 (0.764)	0.609 (0.624)	0.803 (0.816)
0.3	0.798 (0.805)	0.617 (0.635)	0.773 (0.789)
0.4	0.824 (0.830)	0.618 (0.638)	0.750 (0.774)
0.5	0.841 (0.847)	0.615 (0.639)	0.731 (0.754)

TABLE 3. WIDE-BAND ALBEDO OF VERTICALLY INHOMOGENEOUS CLOUD $R(ih)$ AND ITS HOMOGENEOUS COUNTERPART $R(h)$ IN TROPICAL AND MID-LATUTIDE SUMMER ATMOSPHERES

	Tropics		Mid-latitude summer	
Band (cm^{-1})	13 333–40 000	2500–13 333	13 333–40 000	2500–13 333
Band (μm)	0.25–0.75	0.75–4.00	0.25–0.75	0.75–4.00
$R(h)$	0.764	0.624	0.765	0.623
$R(ih)$	0.758	0.609	0.758	0.609
ΔR	−0.006	−0.015	−0.007	−0.014

$\Delta R = R(ih) - R(h)$. Cloud with $\langle w \rangle = 0.2$ ($g\ m^{-3}$), $\langle N \rangle = 50$ (cm^{-3}); $\theta_0 = 0°$ (see text for explanation of symbols).

cases. Five different values of $\langle w \rangle$ are considered. The other cloud microphysical properties and θ_0 are kept the same as those for Fig. 9(a). It is seen that, while the inhomogeneous case always has a lower near-infrared albedo, the actual difference in the near-infrared albedo with respect to the homogeneous case is small. The difference in the ratio of the near-infrared to visible albedo between the inhomogeneous and homogeneous cases for the LWCs considered is less than 4%, with a smaller value for the inhomogeneous cloud.

We have also considered similar cloud cases in the mid-latitude summer atmosphere. We find that the spectral reflectance features exhibit differences between the two cloud cases that are very similar to those seen for tropical conditions. A comparison of the reflectances averaged in the visible and near-infrared spectra is listed in Table 3. As seen earlier for the tropical atmosphere, there is lesser reflectance in the near-infrared region for inhomogeneous clouds. Just like for cloud absorption (Table 1), Table 3 indicates very little influence due to the atmospheric profile on the difference between the inhomogeneous and the equivalent homogeneous cloud albedos.

Hignett (1987) found that the cloud albedo observed is close to the theoretical calculation in the visible region but is significantly less than the calculated results in the near-infrared region. The ratio of near-infrared to visible albedo is estimated to be about 10% less than the theoretical evaluation. Hignett's theoretical results were derived from plane-parallel calculations. In his calculations, the vertically accumulated LWC is used to obtain the liquid-water path (LWP), with consideration of the maximum and minimum values of LWP. The values of single-scattering albedo and backscattering fraction (asymmetry factor) were tuned to match the results of more precise calculations. It is not apparent whether the vertical variations of LWC and the concomitant single-scattering albedo and asymmetry factor were explicitly accounted for. The difference between the calculated and observed values of the near-infrared albedo in that study has been claimed as a possible

evidence of cloud absorption anomaly (Stephens and Tsay 1990). Our study shows that the difference in cloud near-infrared albedo may be attributable, at least in part, to a simple physical reason: the cloud internal distribution of the microphysical properties. However, considering the spectrally integrated value of the near-infrared band, the difference due to cloud vertical inhomogeneity is too small to explain entirely the results of Hignett (1987).

In this context, it must also be mentioned that the definition and computation of the near-infrared albedo is sensitive to the water vapour distribution above the cloud (Davies *et al.* 1984; Ramaswamy and Freidenreich 1992). This is because the solar irradiance actually incident on the top of low clouds (homogeneous or inhomogeneous) is considerably different in its spectral distribution than that at the top of the atmosphere. Since the near-infrared regime has attenuation by both drops and vapour, the determination of, and inferences concerning, broadband albedo of any cloud case are consequently sensitive to this particular point. This point is not to be confused with the specific issue of differences between homogeneous and inhomogeneous clouds which, in the present work, are found to be quite similar for the tropical and mid-latitude summer atmospheric profiles. In contrast to the effects of vertical inhomogeneity in clouds, it is pointed out that aerosols and large drop distributions (Wiscombe *et al.* 1984), two potential factors that have been suggested in the cloud solar-absorption-anomaly problem (Stephens and Tsay 1990), are unlikely to explain completely the albedo discrepancies in the near-infrared spectrum reported by Hignett (1987). This is because both these factors are likely to cause a significant change in the visible spectrum albedos as well, which is not observed.

Recent measurements by Hayasaka *et al.* (1995) show that the measured ratio of near-infrared to visible albedos are close to theoretical calculations for clouds with horizontally homogeneous structure. The measured ratios of near-infrared to visible albedo are lower (by about 10%) than calculated results only for clouds with horizontally inhomogeneous structure. Our results are consistent with the conclusion of Hayasaka *et al.* (1995) for horizontally homogeneous clouds.

4. Conclusions

Cloud liquid-water content can increase by about 2 orders of magnitude from cloud bottom to cloud top, which represents a substantial departure from the assumption of a cloud layer with homogeneous microphysical properties. The impact of this feature on radiative transfer (cloud absorption and reflection) has been investigated using the GFDL line-by-line solar radiative-transfer model combined with a new 4-stream method for handling multiple scattering. A modified gamma distribution is assumed for cloud droplets, and a general relationship between liquid water content and effective radius is obtained using physical bases.

By itself, the vertical variation of droplet microphysics leads to a higher absorption for the inhomogeneous cloud case relative to the homogeneous counterpart, with the absorption occurring primarily at wave numbers less than 8000 cm^{-1} (wavelengths greater than 1.25 μm). The presence of water vapour can partly offset the enhancement of cloud absorption that is obtained due to the vertical inhomogeneity in the drop microphysical properties. LWC is an important determinant of the quantitative differences introduced by vertical inhomogeneity in clouds. In contrast, changes in the value of the number concentration and its vertical slope have a relatively smaller influence on the differences between the inhomogeneous and the equivalent homogeneous cloud cases. Considering a typical stratus or a stratocumulus cloud with a vertically averaged LWC of about 0.2 g m^{-3}, a calculation assuming a realistic inhomogeneous distribution of the cloud microphysics absorbs more, but not substantially more, solar radiative energy than one in which the

properties are homogeneous. However, the vertical distribution of heating rate inside the cloud is changed dramatically, with a substantial increase in the top region of the cloud for the inhomogeneous case. The relatively larger heating rate near the top of the cloud may have an important impact on cloud formation and maintenance processes and is, hence, of particular interest in cloud-modelling studies.

The presence of vertical inhomogeneity in microphysics can reduce the cloud albedo by more than 10% at wave numbers less than 10 000 cm^{-1} (wavelengths greater than 1 μm). The decrease in the near-infrared albedo for inhomogeneous clouds is a robust feature of our calculations, regardless of the cloud liquid-water path and solar zenith angle. However, the frequency-integrated albedo difference caused by the cloud vertical inhomogeneity is too small to explain the observations of Hignett (1987), even though it is of the right sign.

Acknowledgements

We are grateful to S. M. Freidenreich for help with the model and fruitful discussions. We also thank B. J. Soden and C. T. Gordon for their remarks and suggestions. The anonymous reviewers and the Associate Editor (K. P. Shine) are thanked for their helpful comments on the paper.

References

Barker, H. W. and Davies, J. A. 1992 Solar radiative fluxes for a stochastic, scaling invariant broken cloud field. *J. Atmos. Sci.*, **49**, 1115–1126

Coakley, J. A., Cess, R. D. and Yurevich, F. B. 1983 The effects of tropospheric aerosols on the Earth's radiation budget; A parameterization for climate models. *J. Atmos. Sci.*, **40**, 116–138

Coakley, J. A., Bernstein, R. L. and Durkee, P. A. 1988 Pp. 253–260 in *Aerosols and climate*. Eds. P. V. Hobbs and M. P. McCormic. A Deepak publishing

Davies, R. 1978 The effect of finite geometry on the three-dimensional transfer of solar irradiance in clouds. *J. Atmos. Sci.*, **35**, 1712–1725

Davies, R., Ridgway, W. L. and Kim, K.-E. 1984 Spectral absorption of solar radiation in a cloudy atmosphere: a 20 cm^{-1} model. *J. Atmos. Sci.*, **41**, 2126–2137

Freidenreich, S. M. and Ramaswamy, V. 1993 Solar radiation absorption by CO_2, overlap with HO_2, and a parameterization for general circulation models. *J. Geophys. Res.*, **98**, 7255–7264

Hayasaka, T., Nakajima, T., Fujiyoshi, Y., Ishizaka, Y., Takeda, T. and Tanaka, M. 1995 Geometrical thickness, liquid water content, and radiative properties of stratocumulus clouds over the western North Pacific. *J. Appl. Meteorol.*, **34**, 460–470

Hignett, P. 1987 A study of the short-wave radiative properties of marine stratus: Aircraft measurements and model comparisons. *Q. J. R. Meteorol. Soc.*, **113**, 1011–1024

Hunt, G. E. and Grant, I. P. 1969 Discrete space theory of radiative transfer and its application to problems in planetary atmospheres. *J. Atmos. Sci.*, **26**, 963–972

Li, J. and Ramaswamy, V. 1996 Four-stream spherical harmonic expansion approximation for solar radiative transfer. *J. Atmos. Sci.*, **53**, 1174–1186

Li, J., Geldart, D. J. W. and Chýlek, P. 1994 Solar radiative transfer in clouds with vertical internal inhomogeneity. *J. Atmos. Sci.*, **51**, 2542–2552

Mason, B. J. 1971 *The physics of clouds*. Clarendon Press, Oxford

McClatchey, R. A., Fenn, R. W., Selby, J. E. A., Volz, F. E. and Garing, J. S. 1972 'Optical properties of the atmosphere'. Report AFCRL-72-0497. Hanscom Air Force Base, Bedford, Mass., USA

McKee, T. B. and Cox, S. K. 1974 Scattering of visible radiation by finite clouds. *J. Atmos. Sci.*, **31**, 1885–1892

Noonkester, V. R. 1984 Droplet spectra observed in marine stratus cloud layers. *J. Atmos. Sci.*, **41**, 829–845

Paltridge, G. W. 1974 Infrared emissivity, short wave albedo, and the microphysics of stratiform water clouds. *J. Geophys. Res.*, **79** (27), 4053–4058

Platt, C. M. R.	1976	Infrared absorption and liquid water content in stratocumulus clouds. *Q. J. R. Meteorol. Soc.*, **102,** 515–522
Ramaswamy, V. and Freidenreich, S. M.	1991	Solar radiative line-by-line determination of water vapor absorption and water cloud extinction in inhomogeneous atmospheres. *J. Geophys. Res.*, **96,** 9133–9157
	1992	A study of broadband parameterizations of the solar radiative interactions with water vapor and water drops. *J. Geophys. Res.*, **97,** 11487–11512
Rothman, L. S., Gamache, R. R., Barbe, A., Goldman, A., Gillis, J. R., Brown, L. R., Toth, R. A., Flaud, J. M. and Camy-Perot, C.	1983	AFGL atmospheric absorption line parameter compilations: 1982 edition. *Appl. Opt.*, **22,** 2247–2256
Slingo, A.	1989	A GCM parameterization for the shortwave radiative properties of water clouds. *J. Atmos. Sci.*, **47,** 1419–1427
Slingo, A., Brown, R. and Wrench, C. L.	1982a	A field study of nocturnal stratocumulus. III: High-resolution radiative and micro-physical observations. *Q. J. R. Meteorol. Soc.*, **108,** 145–165
Slingo, A., Nicholls, S. and Schmetz, J.	1982b	Aircraft observations of marine stratocumulus during JASIN. *Q. J. R. Meteorol. Soc.*, **108,** 833–856
Stephens, G. L.	1978	Radiation profiles in extended clouds. Part I: Theory. *J. Atmos. Sci.*, **35,** 2111–2122
Stephens, G. L. and Platt, C. M. R.	1987	Aircraft observations of the radiative and microphysical properties of stratocumulus and cumulus clouds fields. *J. Climatol. Appl. Meteorol.*, **26,** 1243–1269
Stephens, G. L. and Tsay, S. C.	1990	On the cloud absorption anomaly. *Q. J. R. Meteorol. Soc.*, **116,** 671–704
Welch, R. M. and Wielicki, B. A.	1985	A radiative parameterization of stratocumulus cloud fields. *J. Atmos. Sci.*, **42,** 2888–2897
Wiscombe, W. J., Welch, R. M. and Hall, W. D.	1984	The effects of very large drops on cloud absorption. Part I: Parcel models. *J. Atmos. Sci.*, **41,** 1336–1355
World Meteorological Organization	1986	Pp. 355–362 in 'Atmospheric ozone'. WMO Report No. 16, Geneva, Switzerland